

**CYCLONE STRUCTURAL TESTING STATION
JAMES COOK UNIVERSITY**

**WIND LOADS ON FENCES
AND HOARDINGS**

by

J. D. Ginger, G. F. Reardon and B. L. Langtree

TECHNICAL REPORT No 47

September 1998

CYCLONE STRUCTURAL TESTING STATION

WIND LOADS ON FENCES AND HOARDINGS

J. D. Ginger, G. F. Reardon and B. A. Langtree

Abstract

A wind tunnel study was carried out to determine net pressures coefficients (C_{pn}) on fences and hoardings, and identify configurations experiencing large loads. The measured pressures compared favourably with data from other studies. Large mean net pressures were measured on fence panels close to the windward free-end for approach wind directions θ of 30° to 45° . The net pressure coefficients on fence panels close to the windward free-end increased as the aspect ratio (length/height, b/h) was increased to 8 and then decreased slightly as the aspect ratio was increased to 12. Good agreement generally exists between the measured mean net pressure coefficients and AS1170.2 design data on fences and hoardings. AS1170.2 however underestimates loads on windward free-end fence panels for approach wind directions θ of 30° to 45° , and on hoardings with clearance ratios (c/h) of ~ 0.8 . Some codes (i.e. ASCE 7-95) have more significant differences in data.

WIND LOADS ON FENCES AND HOARDINGS

TABLE OF CONTENTS

1	INTRODUCTION	1
2	RELATED MODEL AND FULL-SCALE STUDIES	2
2.1	Wind tunnel studies at CSIRO, Oxford and UQ	2
2.2	Full-scale tests at Silsoe	3
3	EXPERIMENTAL SET UP AT CSTS	4
4	RESULTS	6
4.1	Area averaged panel pressures on fences	6
4.2	Point pressure measurements on fences	13
4.3	Area averaged panel pressures on hoardings	13
5	DESIGN REQUIREMENTS OF FENCES	16
6	CONCLUSIONS	20
7	REFERENCES	20
	APPENDIX A	22

1 INTRODUCTION

Fences range from 1 to 2 m tall boundary walls and 2 to 5m tall traffic noise barriers up to 5 to 10m tall security walls. The type of construction can vary from lightweight timber and metal fences built to ensure privacy, to timber, brick or custom made sound barriers, to thicker more secure block or concrete walls. Hoardings are generally used for advertising and are erected at prominent locations such as alongside highways in isolation or in city centers on other structures.

Fences and hoardings have traditionally been designed and constructed with minimum engineering input, and “accepted styles” have evolved over time. Wind loads are the predominant design loads on fences and hoardings. Non-engineered fences and hoardings are prone to windstorm damage. Many building codes are therefore being updated with wind loading data on fences and hoardings. Previously code data was usually based on a few studies of limited scope, resulting in some errors and discrepancies. Differences in data values provided by various codes have created confusion in the building industry with regards to its application, as described by Robertson et al (1995). A full-scale study on a fence was implemented at Silsoe in England, to address some of these issues. Notwithstanding limitations in this full scale study, such as the fixed orientation of the fence with the predominant wind direction and the maximum length of the fence, it is expected to provide data which could be used to validate the wind tunnel results and update values in codes.

Results from wind tunnel studies carried out by Holmes (1985) at CSIRO in Australia and Letchford (1985) at Oxford in England, in simulated Atmospheric Boundary Layer (ABL) flows were used to update the Australian Standard AS1170.2 (1989), ESDU Data Item 89050 (1989) and the British Standard BS 6399 (1995). Data from these two studies have since been combined in a publication by Letchford and Holmes (1994). Letchford (1998) carried out additional studies on signboards and hoardings at the University of Queensland (UQ). The lack of further reliable data and the increasing use of new materials and innovative techniques applied to the design and construction of wind sensitive fences and hoardings has created a need to further qualify and calibrate design data prescribed in codes.

The fence and hoarding model test configurations are shown in Figure 1.1, and the same terms as those given in AS1170.2 are used in this study. The parameters investigated in this study of fences are the aspect ratio b/h and wind direction θ , and of hoardings (with fixed aspect ratio $b/c = 2$), are the clearance ratio c/h and wind direction θ . This wind tunnel study was therefore carried out to:

- determine the pressure distribution on a range of fence and hoarding configurations
- compare pressure coefficients with data in codes and other model and full-scale data
- identify fence and hoarding configurations and local regions experiencing large loads
- calculate selected load effects using AS1170.2 and wind tunnel data

Section 2 summarizes the previous wind tunnel studies and the full-scale study at Silsoe. The wind tunnel test procedure, model set up and the definitions used in this report are described in Section 3. The pressure coefficients obtained in the wind tunnel study and comparisons with AS1170.2 are given in Section 4. Selected design load effects on a fence are calculated using the wind tunnel data and AS1170.2 in Section 5. The conclusions are presented in Section 6.

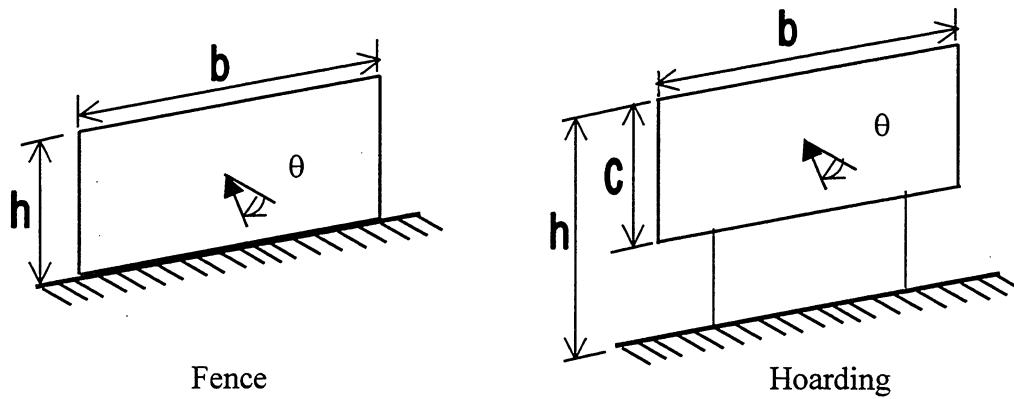


Figure 1.1 Fence and hoarding configurations used in this study

2 RELATED MODEL AND FULL-SCALE STUDIES

Holmes (1985) and Letchford (1985) carried out separate wind tunnel model studies, on fences placed in simulated ABL flows. Wind loads acting on different parts of a full-scale fence are being studied at Silsoe, as described by Robertson et al (1997). Letchford and Robertson (1998) and Letchford (1998) carried out further studies and analyzed and compared the relevant data contained in the literature. Previously, data contained in codes and builders manuals were based on measurements of drag forces on plates in flow conditions that did not always adequately simulate ABL flows. The Jensen No (Je), h/z_0 is the appropriate non-dimensional parameter relating the structure height h and the boundary layer flow characterized by its roughness length z_0 to be considered in a study such as the present one.

Good and Joubert (1968) measured pressure distributions on a 2D fence in smooth-wall turbulent boundary layer flow for various ratios of fence height to boundary layer thickness. Ranga Raju et al (1976) performed measurements on 2D fences of various heights in turbulent boundary layers of several different thicknesses where the ratio of fence height to boundary layer thickness varied from less than 0.05 to greater than unity, and compared the data with other published data. Sakamoto and Arie (1983) measured the drag on fences of aspect ratio (length/height = b/h) between 0.5 and 10, immersed in a smooth-wall turbulent boundary layer, and found that the minimum mean drag coefficient occurred at an aspect ratio of 5. Holmes (1985) analyzed the data of Good and Joubert (1968) and Ranga Raju et al (1976) and found that the mean drag coefficient based on the velocity at the top of the fence was equal to 1.1, and effectively independent of Je ranging from 40 to 1000.

2.1 Wind tunnel studies at CSIRO, Oxford and UQ

Separate wind tunnel model studies on fences were carried out by Holmes (1985) at CSIRO and Letchford (1985) at Oxford, at a length scale of 1/75. The roughness lengths z_0 of the simulated ABL flows were equivalent to full-scale values of 30 mm and 100 mm respectively. For flow over terrain category 2 and 3 as per AS1170.2, z_0 is 20 mm and 200 mm respectively. The mean velocity profiles from both studies were quite similar and matched the target profiles at full-scale heights between 5 m and 20 m. However, below the elevation of 5 m, Letchford's (1985) profile was steeper than Holmes' (1985) and the target mean velocity profiles. At full-scale heights of 5 m and 10 m, Letchford's (1985) tests had turbulence intensities of 0.24 and 0.23 and Holmes (1985) tests had turbulence intensities of 0.21 and 0.19 respectively.

Letchford (1985) tested two model fences equivalent to full-scale heights of 5m and 10m at Oxford. Fifteen pressure taps were installed on areas corresponding to 25 m² and 50 m² respectively on each model to enable pressures on finite areas to be collected. Holmes (1985) tested a fence representing a full-scale height of 4.8 m at CSIRO. Twenty four pressure taps covering an area of 4.8 × 7.2 m² on each face, were manifolded in groups of six so that the area averaged pressures could be measured on four, 2.4 × 3.6 m² discrete areas. The Jensen No, Je were approximately 50 and 100 in the Oxford tests and 160 in the CSIRO tests.

An infinite fence is defined as one which spans the entire width of the wind tunnel, such that the mean pressure coefficients averaged over its height are independent of the position along the fence. A semi-infinite fence spans half the width of the wind tunnel and the mean pressure coefficients averaged over the height depends on the distance from the leading edge and on the width of the area averaging “panel”. Measurements were made on infinite fences, semi-infinite fences and a number of fences of finite length at both Oxford and CSIRO. At Oxford, finite length fences with aspect ratios of 1, 2 and 3 for the shorter (i.e. $h = 5\text{m}$) fence, and 0.5, 1 and 1.5 for the taller (i.e. $h = 10\text{m}$) fence were tested. At CSIRO, finite length fences with aspect ratios of 1.5, 5 and 10 were tested.

Letchford (1998) also measured the normal force coefficients on a range of rectangular signboards and hoardings at the University of Queensland (UQ). These wind tunnel model tests were carried out using a force balance at a length scale of 1/50. The models ranged from 50 × 50 mm² to 100 × 400 mm² with the clearance beneath the panels extending from 5 mm to 150 mm. His detailed parametric study investigated the effects of aspect ratio, clearance ratio and porosity for a range of wind directions. He presented a simple expression for the normal force coefficient C_f (i.e. net pressure coefficient) by Equation 2.1, for panels $0.2 < b/c < 5$ and $0.2 < c/h < 1.0$.

$$C_f = 1.45 + 0.5(0.7 + \log(b/c))(0.5 - (c/h)) \quad 2.1$$

2.2 Full-scale tests at Silsoe

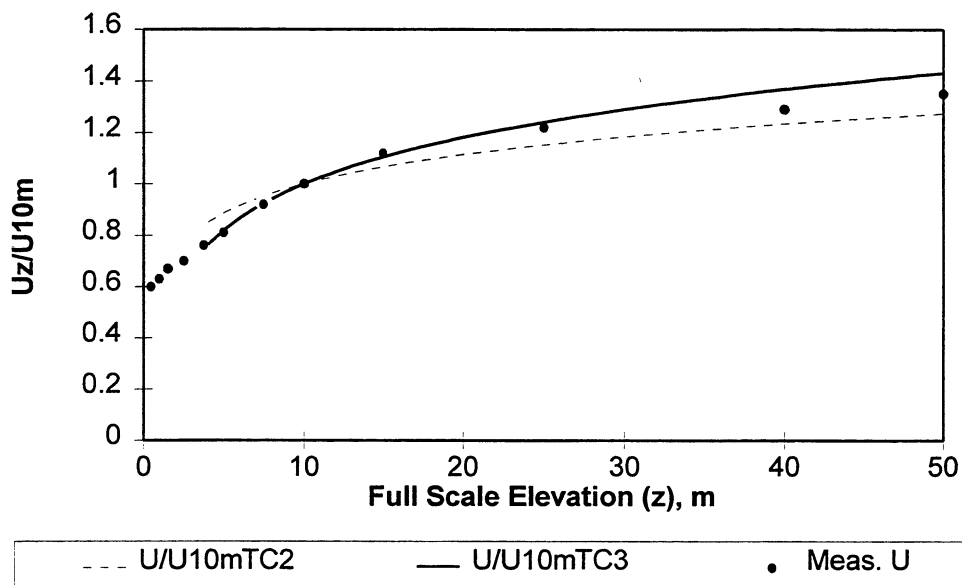
Significant increases in wind loads obtained from model studies by Letchford (1985) and Holmes (1985) have since been incorporated in to the Australian Wind Loading Standard AS1170.2 (1989) and British Standard BS 6399 (1995). Similar values are also contained in the ENV 1991-2-4, Eurocode 1: (1994). Concerns over these large increases on the free-end panel and contradictory values given in other codes were partly responsible for the full-scale fence study at Silsoe.

The full-scale fence set up at Silsoe was described by Robertson et al (1997). The fence is 2m high (h) and 215 mm thick, and data is collected over an instrumented 2m wide panel containing fifteen taps. This panel can be moved within the wall whose maximum length is 13h. The net pressure coefficients are referenced to the mean dynamic pressure at fence height, obtained from instruments located upstream. The approach flow is over open grassland with $z_0 = 0.01\text{m}$, and the turbulence intensity at fence height of 2m is ~ 20%.

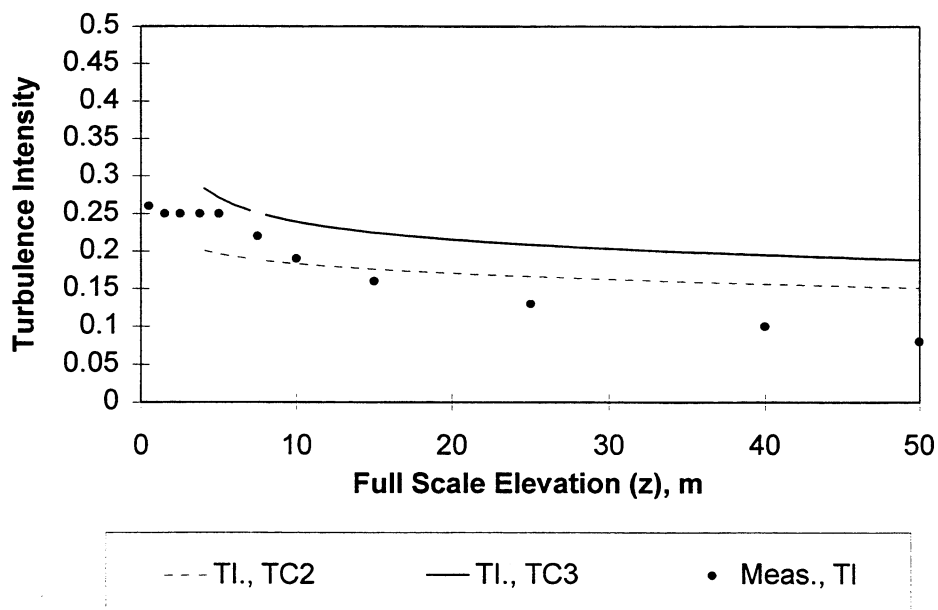
As described by Robertson et al (1997), the issues being addressed in this full-scale study are the effect of aspect ratio (b/h) on the end and middle panel loads, the effect of corner configuration on the end panel wind loads and the effect of gaps in the fence. Measurements by Robertson et al (1997) indicated an increasing mean normal force coefficient (i.e. net pressure coefficient) with increasing aspect ratio, up to the longest possible fence of length $b = 13h$. Additional wind tunnel studies are therefore required to determine the variation of normal force coefficient (or net pressure coefficient) with a range of fence aspect ratios including those that have not been tested.

3 EXPERIMENTAL SET UP AT CSTS

This study was carried out by the Cyclone Structural Testing Station (CSTS), in the 2.5m wide \times 2m tall \times 22m long Boundary Layer Wind Tunnel at the School of Engineering, James Cook University. The approach ABL was simulated at a length scale of 1/50 over the upstream fetch using a 250 mm high trip board at the upstream end followed by an array of blocks on the tunnel floor. Figure 3.1 shows that the mean velocity and turbulence intensity profiles measured at the working section fall between AS1170.2 terrain category 2 and 3 profiles. The longitudinal length scale of turbulence in this study was estimated to be smaller than the target value by a factor of about 3, which is considered an acceptable degree of relaxation for such a wind tunnel study.



(a) Mean Velocity



(b) Turbulence Intensity

Figure 3.1 Simulated Atmospheric Boundary Layer at a length scale of 1/50

A 80 mm high \times 160 mm long \times 8 mm thick pressure tapped model panel shown in Figure 3.2 was constructed in sandwich form consisting of front and rear faces. At a length scale of 1/50, this represents a 4 m tall \times 8 m long \times 0.4 m thick full-scale panel. Each face contains sixteen (16) evenly spaced taps positioned opposite each other such that the net (front-rear) pressures can be measured. This pressure tapped panel was installed at selected positions along with blank panels in fences of varying lengths. This enables the determination of the pressures on different parts (i.e. middle, free-end) of these fences. The pressure tapped panel was mounted on legs to determine the pressures on hoardings located clear of the ground. The effect of hoarding elevation above ground and clearance between hoarding and ground was determined by changing the height of these legs. The pressures were measured for approach wind directions θ of -90° through 0° to 90° , in 15° steps.

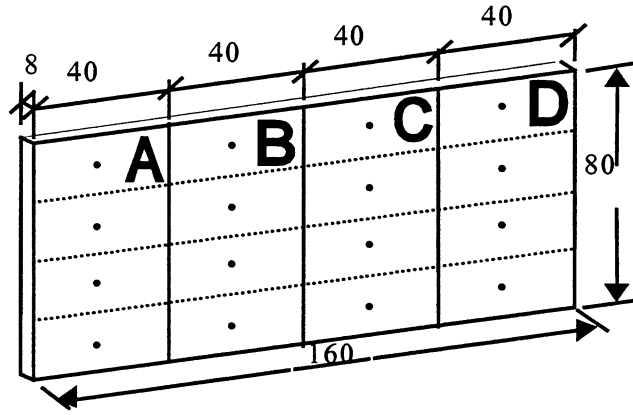


Figure 3.2. 80 mm high \times 160 mm long \times 8 mm thick pressure tapped model panel • Taps

The pressures were measured using 600 mm long, 1.5 mm diameter tube-restrictor system connected to pressure transducers via Scanivalves. Front and rear face tap pressures were differenced to give net (front-rear) pressure. These fluctuating pressures were filtered at 250 Hz corresponding to a full-scale frequency of 10 Hz. This data was sampled at 500 Hz, for 24 sec corresponding to 10 mins in full scale using a PC controlled data acquisition system, and statistically analyzed to give mean, standard deviation, maximum and minimum pressures. Pressure measurements were repeated for 5 runs for each configuration and averaged.

The mean, standard deviation, maximum and minimum net (front-rear) pressure coefficients referenced to the mean dynamic pressure at the top of the fence or the top of the hoarding of height h are defined respectively as;

$$C_{\bar{p}_n} = \bar{p}_n / \left(\frac{1}{2} \rho \bar{U}_h^2 \right), \quad C_{\sigma p_n} = \sigma p_n / \left(\frac{1}{2} \rho \bar{U}_h^2 \right), \quad C_{\hat{p}_n} = \hat{p}_n / \left(\frac{1}{2} \rho \bar{U}_h^2 \right), \quad C_{\check{p}_n} = \check{p}_n / \left(\frac{1}{2} \rho \bar{U}_h^2 \right)$$

The area averaged mean pressures over $h/2$ wide panels identified as A, B, C and D were obtained by averaging the mean pressures collected at the four taps in each area shown in Figure 3.2.

In this study, the maximum blockage (i.e. projected area of model to wind tunnel cross sectional area) was of $\sim 1.5\%$, for which corrections to the pressures are small and were therefore neglected. The percentage variability of the area averaged mean pressure on a panel for oblique approach wind directions, defined in terms of the standard deviation of the data set divided by the mean, over 5 runs was typically 2 to 3%.

4 RESULTS

Point and area averaged net pressures obtained by the CSTS over a range of fences and hoardings are analyzed in this section and compared with other data. Previous studies by Letchford (1985) indicated that the loading on fence and hoarding panels behaved quasi-statically, and hence the results of this study concentrate on mean pressures. In cases where the fence and hoarding configurations were similar and other parameters (i.e. aspect ratio, panel size) were comparable, quantitative comparisons are made between the CSIRO, Oxford, Silsoe, UQ and CSTS studies and the data given in codes (i.e. AS1170.2, ENV 1991-2-4, ASCE 7-95 and ISO 4354).

4.1 Area averaged panel pressures on fences

The pressures on fences of finite length depend on the aspect ratio of the fence, wind direction, location of the panel from the free-end and the width of the panel. In tests at CSTS, the pressure tapped fence panels defined A, B, C and D were h (i.e. 4m in full-scale) high \times $h/2$ wide. The variation of area averaged mean net pressure coefficients on panels A, B, C and D with wind direction θ , with the pressure tapped panels placed in the middle of the fence (denoted by subscript M) and at an end (denoted by subscript E) such that panel A is at the free-end, for fences of aspect ratios 2, 4, 6, 8 and 12 and AS1170.2 data are given in Tables A1 to A9 in Appendix A. Figures 4.1 to 4.9 show this variation of mean loads on each panel. For those tests in which the pressure tapped panels were in the middle of the fence, the approach wind direction θ was varied from 0° (i.e. normal to fence) to 90° (parallel to fence). For those tests in which the pressure tapped panels were at the end of the fence, θ was varied from -90° (i.e. parallel to fence with panel A at the trailing end) to 90° (parallel to fence with panel A at the leading end). The results of these tests on fences of finite length are also divided into those that provide loads on the entire fence and those that give loads on selected parts such as the free-end of the fence.

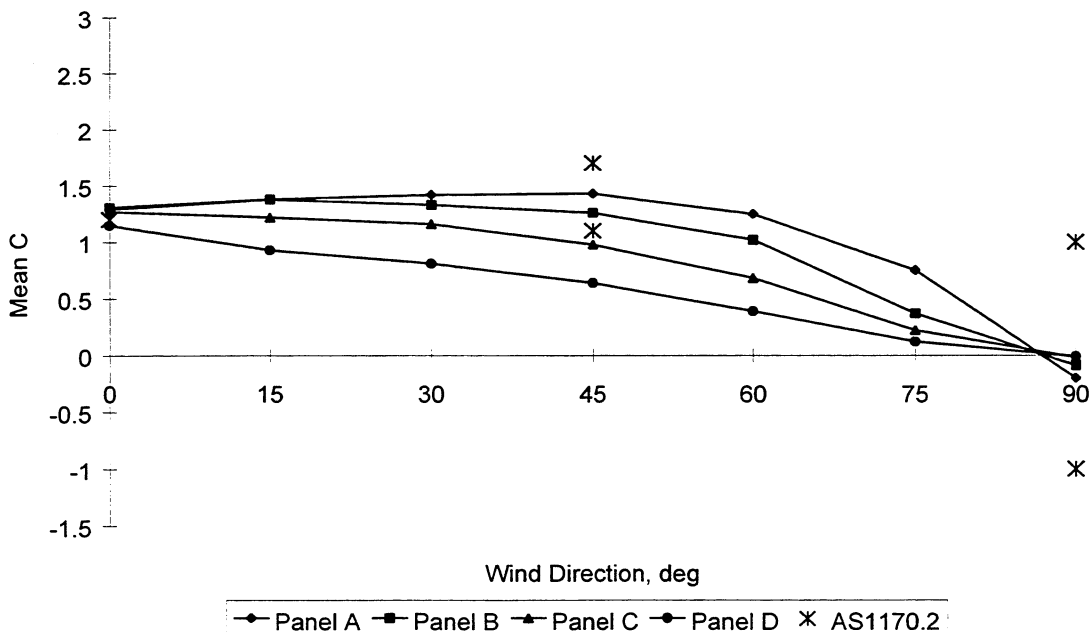


Figure 4.1. C_{pn} vs θ on fence panels $b/h = 2$

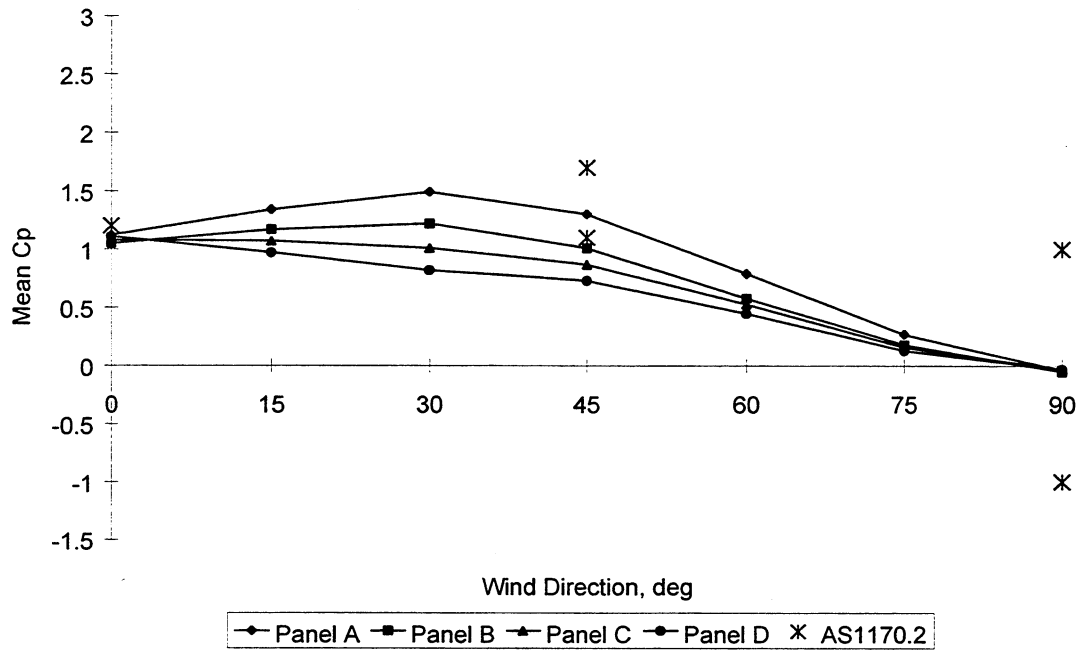


Figure 4.2. C_{pn} vs θ on fence panels in middle section $b/h = 4$

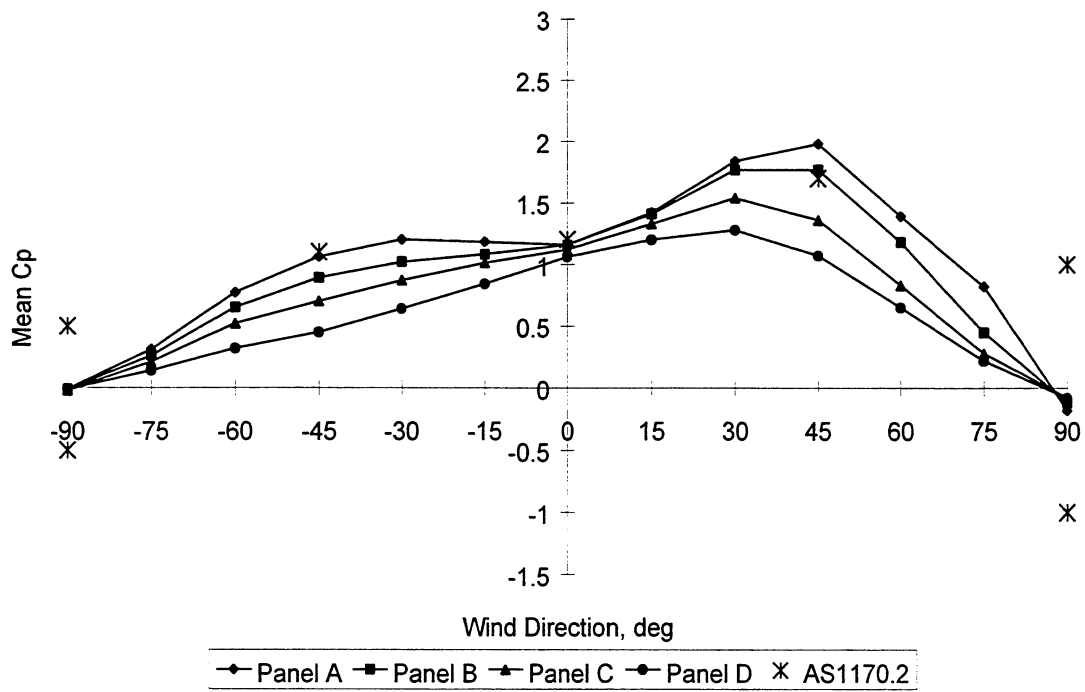


Figure 4.3 C_{pn} vs θ on fence panels in free-end section $b/h = 4$

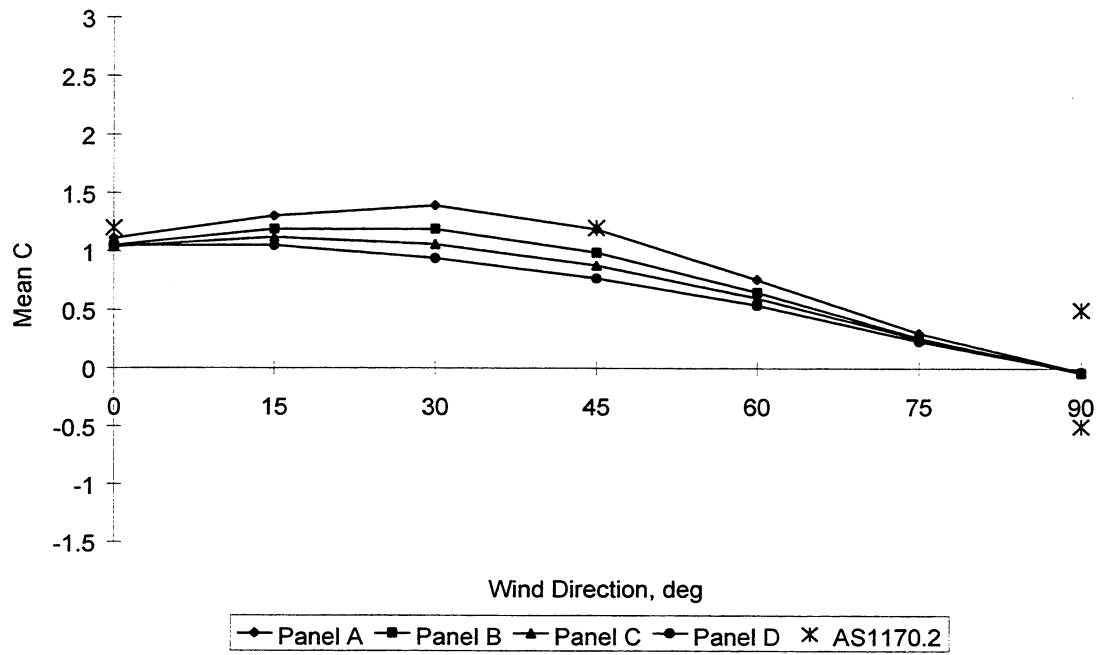


Figure 4.4 C_{pn} vs θ on fence panels in middle section $b/h = 6$

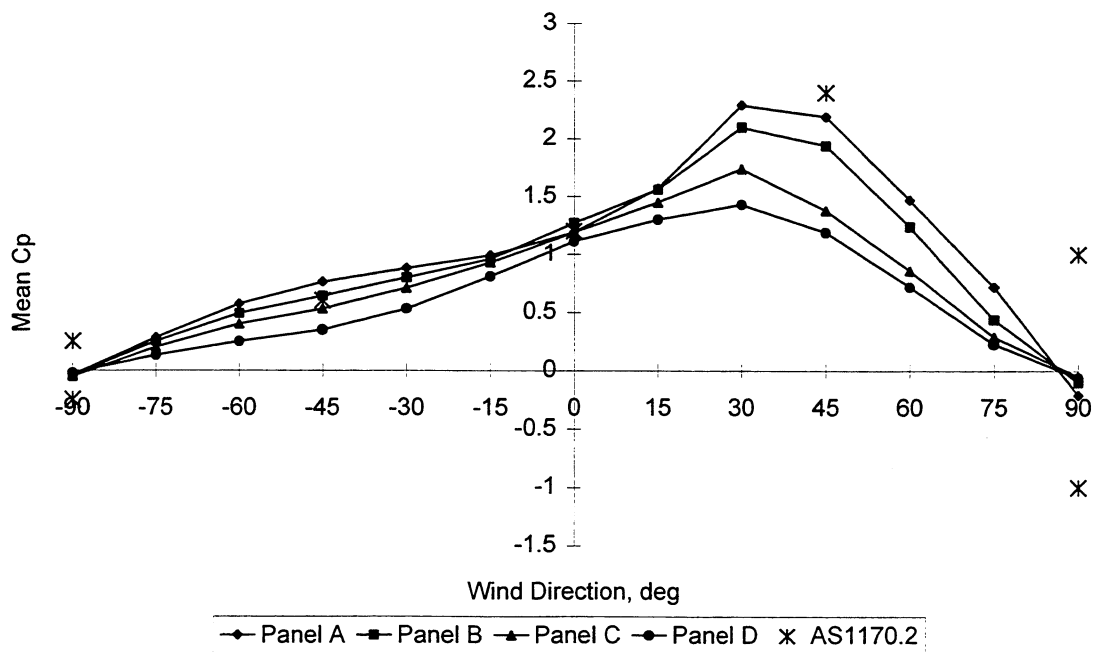


Figure 4.5 C_{pn} vs θ on fence panels in free-end section $b/h = 6$

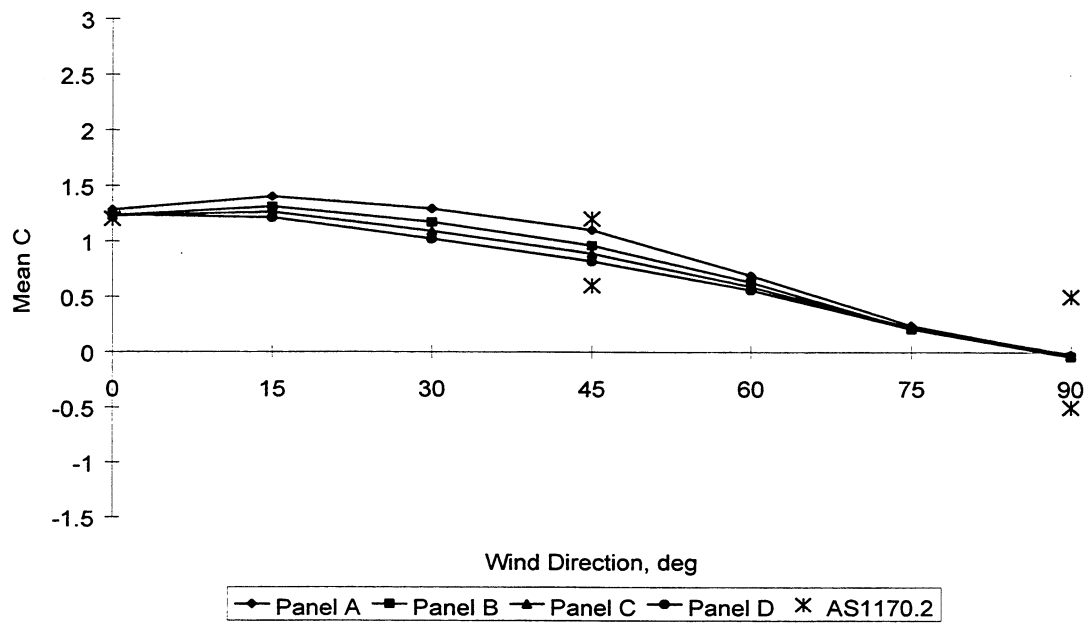


Figure 4.6 C_{pn} vs θ on fence panels in middle section $b/h = 8$

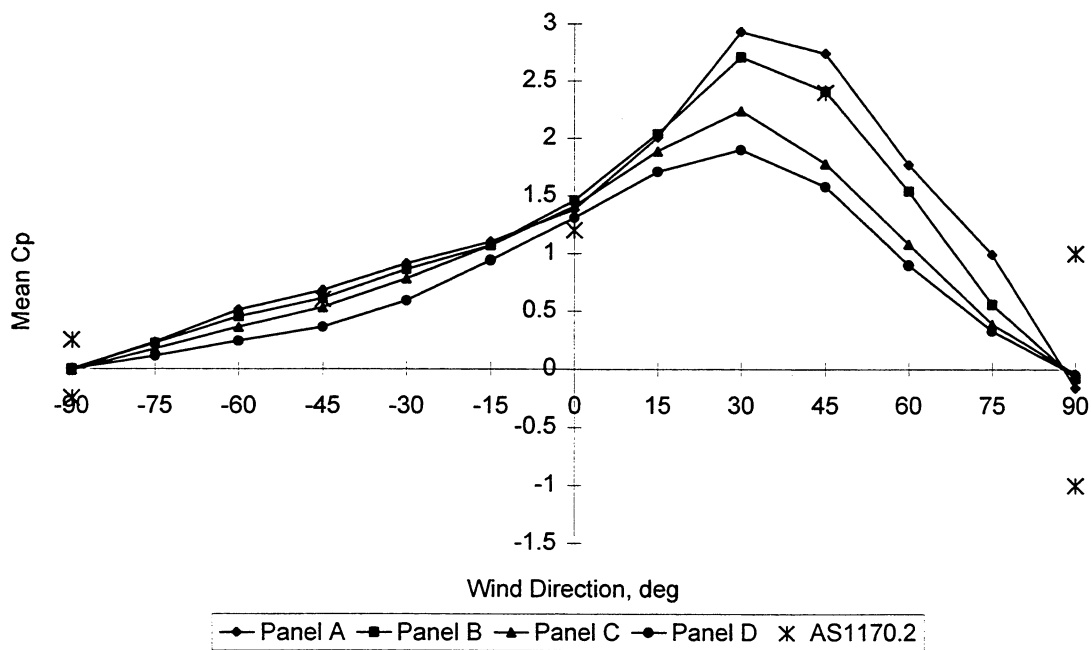


Figure 4.7 C_{pn} vs θ on fence panels in free-end section $b/h = 8$

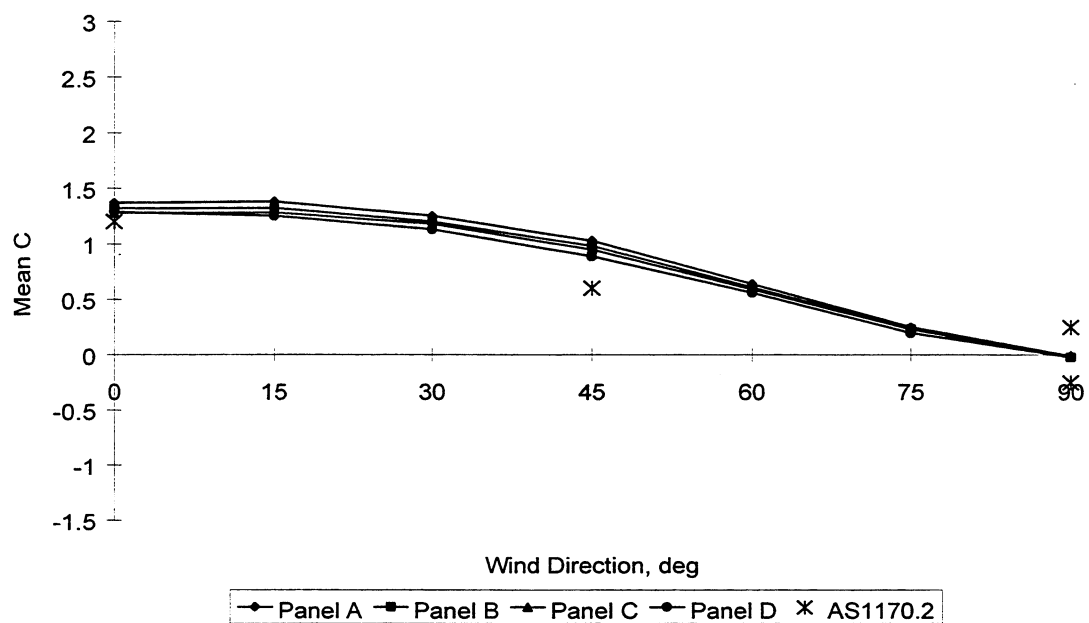


Figure 4.8 C_{pn} vs θ on fence panels in middle section $b/h = 12$

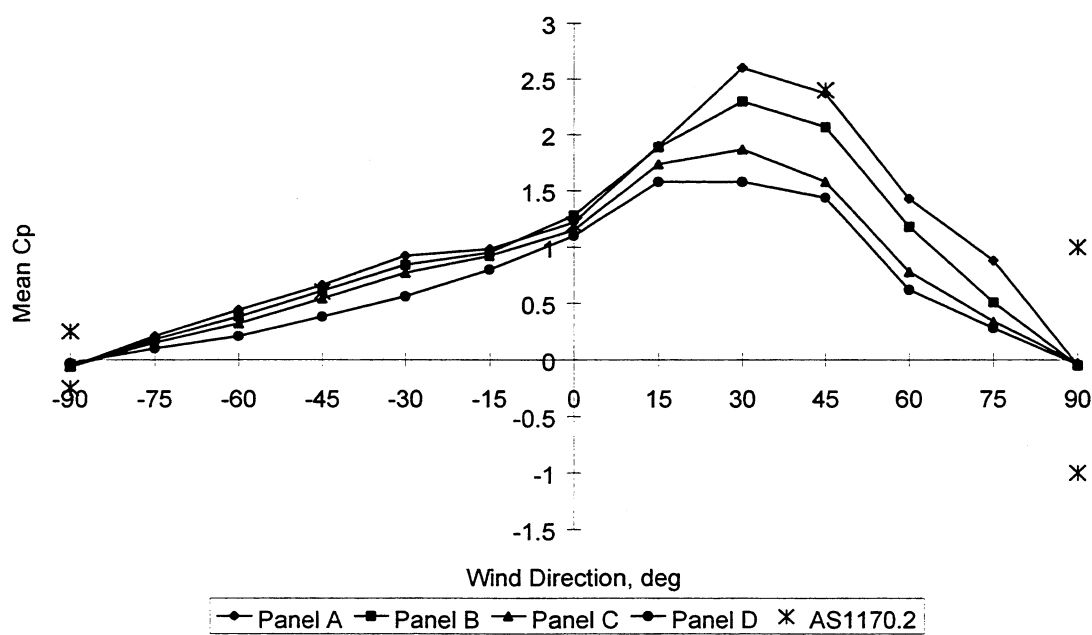


Figure 4.9 C_{pn} vs θ on fence panels in free-end section $b/h = 12$

Figures 4.1 to 4.9 show that the pressure coefficients depend on the aspect ratio of the fence and wind direction. Wind directions θ of 30° to 45° , produce the largest net pressures on the panels adjacent to the windward free-end, which then drop off significantly for $\theta > 60^\circ$. The mean net pressure coefficients increase with aspect ratio and reaches a maximum value of ~ 3 on Panel A, for a fence of aspect ratio 8, and then decreases as the aspect ratio increased to 12. The mean net pressure coefficients also decrease in magnitude with increasing distance away from the windward free-end. Figures 4.3, 4.7 and 4.9 show that the pressure coefficients given in AS1170.2 are smaller than the mean net pressure coefficients measured on Panels A and B near the windward free-end for $\theta = 30^\circ$ to 45° , on fences of aspect ratio of 4, 8 and 12. The fluctuating velocities create positive and negative net loads for flow parallel to the fence (i.e. $\theta = 90^\circ$), which is accounted for in AS1170.2 by alternative positive and negative pressure coefficients.

Variation of the mean net pressure coefficients over the entire fence with aspect ratio, for $\theta = 0^\circ$ obtained from CSIRO, Oxford, Silsoe, UQ and CSTS are given in Table 4.1. Table 4.1 indicates a minimum in mean net pressure coefficients for aspect ratio, b/h of about 5 in all studies. This is similar to that observed by Sakamoto and Arie (1983). The values obtained in the Oxford tests for $\theta = 0^\circ$ were larger than those from CSIRO and the value of $C_f = 1.1$ derived by Holmes (1985). The CSTS tests produced values that were similar to those from the other model studies but larger than the values obtained from the Silsoe full-scale study.

Table 4.1 Comparisons of area averaged mean net pressure coefficients on the entire fence, $\theta = 0^\circ$

Aspect Ratio(b/h)	Area Averaged Mean Pressure Coefficient					
	Letchford & Holmes (1994)		Letchford & Robertson (1998)		Letchford (1998)	Present
	CSIRO	Oxford	Silsoe	Oxford	UQ	CSTS
1		1.33	1.06	1.24	1.15	
1.5	1.17					
2		1.24			1.14	1.25
3		1.22	0.96			
4					1.08	1.12
5	1.07		~ 0.97	1.17	1.04	
6						1.15
7				1.13		
9			~ 0.98	1.16		
10	1.13					
∞	1.21	1.32				

The mean net pressure coefficients averaged over 0.5h, 0.75h, 1h and 1.5h wide panels located immediately adjacent to the free-end on fences of aspect ratios ranging from 1 to 13 from Oxford, CSIRO, Silsoe and CSTS tests, and codes (i.e. AS1170.2 and ENV 1991-2-4) for $\theta = 0^\circ$ and $\theta = 45^\circ$ are given in Tables 4.2 and 4.3 respectively. For $\theta = 0^\circ$ and $\theta = 45^\circ$, ASCE 7-95 gives a value of 1.2 but specifies that the forces act on the vertical line passing through the geometric center and at a distance of $0.2b$ from the vertical line passing through the geometric center, and ISO 4354 gives values ranging from 1.1 to 1.5 for aspect ratios of 1, 10 and ∞ .

Table 4.2 Area averaged net pressure coefficients on free-end fence panels for $\theta = 0^\circ$

Aspect Ratio (b/h)	End Panel Width	CSIRO	Oxford	CSTS	AS1170.2	ENV 1991-2-4	Silsoe
1	0.5h		1.31		1.2	2.88	
	1h		1.33		1.2	2.49	1.1
1.5	0.5h		1.23		1.2	2.88	
	0.75h	1.13			1.2	2.62	
2	1h		1.24	1.25	1.2	2.49	
	1.5h			1.27	1.2	2.36	
3	1h		1.20		1.2	2.49	1.1
	1.5h				1.2	2.36	
4	1h			1.16	1.2	2.49	
	1.5h			1.15	1.2	2.36	
5	1h				1.2	2.49	1.1
	1.5h	1.10			1.2	2.36	
6	1h			1.23	1.2	2.49	
	1.5h			1.22	1.2	2.36	
8	1h			1.42	1.2	2.49	
	1.5h			1.42	1.2	2.36	
9	1h				1.2	2.49	1.1
10	1.5h	1.19			1.2	2.36	
12	1h			1.25	1.2	2.49	
13	1h				1.2	2.49	1.1

Table 4.3 Area averaged net pressure coefficients on windward free-end fence panels for $\theta = 45^\circ$

Aspect Ratio (b/h)	End Panel Width	CSIRO	Oxford	CSTS	AS1170.2	ENV 1991-2-4	Silsoe
1	0.5h		1.34		1.7	2.88	
	1h		1.13		1.4	2.49	0.95
1.5	0.5h		1.50		1.7	2.88	
	0.75h	1.36			1.7	2.62	
2	1h		1.55	1.35	1.7	2.49	
	1.5h			1.22	1.5	2.36	
3	1h		1.87		1.7	2.49	1.60
	1.5h				1.7	2.36	
4	1h			1.88	1.7	2.49	
	1.5h			1.69	1.7	2.36	
5	1h				2.4	2.49	2.10
	1.5h	1.89			2.4	2.36	
6	1h			2.07	2.4	2.49	
	1.5h			1.84	2.4	2.36	
8	1h			2.58	2.4	2.49	
	1.5h			2.31	2.4	2.36	
9	1h				2.4	2.49	1.5
10	1.5h	2.27			2.4	2.36	2.55
12	1h			2.22	2.4	2.49	
13	1h				2.4	2.49	2.70

Table 4.2 for $\theta = 0^\circ$, shows that the mean net pressure coefficient on the free-end panels decrease as the aspect ratio increases to 5, then increases as the aspect ratio was increased to 8, and then decreases slightly as the aspect ratio was increased to 12. Table 4.3 for $\theta = 45^\circ$, shows that the mean net pressure coefficient on the free-end panels increase as the aspect ratio increases to 8, and then decreases slightly as the aspect ratio was increased to 12. Letchford and Robertson (1998) compared the Silsoe full-scale tests and wind tunnel tests at Oxford, and showed that the full-scale mean net pressure coefficients were smaller than the model test values, especially for $\theta = 0^\circ$. They also showed that a regression between full-scale and model results indicated that the wind tunnel results were about 6% larger than full-scale values even after blockage corrections were made.

4.2 Point Pressure Measurements on Fences

Point net pressure distributions obtained over the height of the fence may be used to determine the center of pressure and to estimate the overturning moments at various sections along the fence. Figure 4.10 shows the variation of mean, standard deviation and maximum point net pressure coefficients over the height z of the fence of aspect ratio of 6, for $\theta = 30^\circ$, at $y/h = 0.25$ (windward free-end region), and 2.75 (middle region), where y is measured from the free-end along the fence.

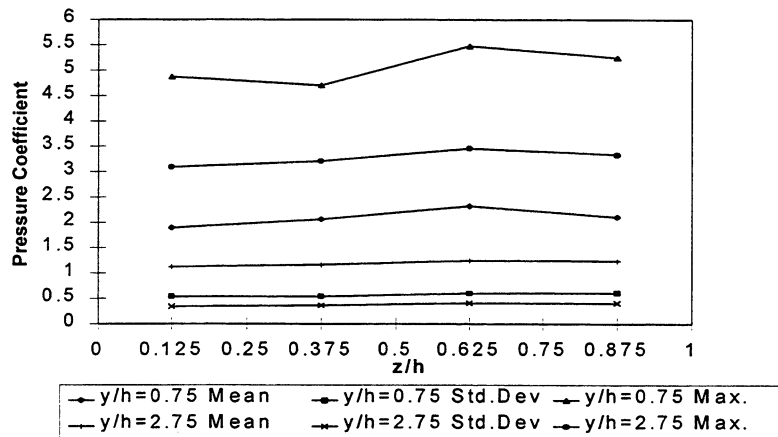


Figure 4.10 Net pressure coefficients vs z/h at various distances y/h along fence, $b/h = 6$ $\theta = 30^\circ$

At every y/h section, the mean and peak net pressure coefficients increase with elevation up to $z = 0.625h$, then decrease at $z = 0.875h$. This distribution is different to that obtained by Letchford (1985) at Oxford in which the pressures were reasonably uniform with height apart from very close to the free end ($y/h = 0.17$). The center of pressure in this CSTS study was estimated to be at $z \sim 0.6h$ whereas in the Oxford tests the center of pressure was just below mid height ($z = 0.49h$). This may be due to the increased roughness and rate of velocity reduction with height in the CSTS tests compared to Oxford. Similar characteristics were also found in the envelopes of standard deviation and peak pressures. For all values of y/h , the largest peak net pressure coefficient occurs at $z/h \approx 0.7$. At Silsoe, Robertson et al (1997) found that the center of pressure was within $z = (0.5 \pm 0.05)h$.

4.3 Area Averaged Panel Pressures on Hoardings

The variation of area averaged mean net pressure coefficients on panels A, B, C and D with wind direction on hoardings (with a fixed aspect ratio $b/c = 2$) for clearance ratios c/h of 0.57, 0.67 and 0.80, and the AS1170.2 values are given in Tables A.10 to A.12 in Appendix A. This data is also shown in Figures 4.11 to 4.13.

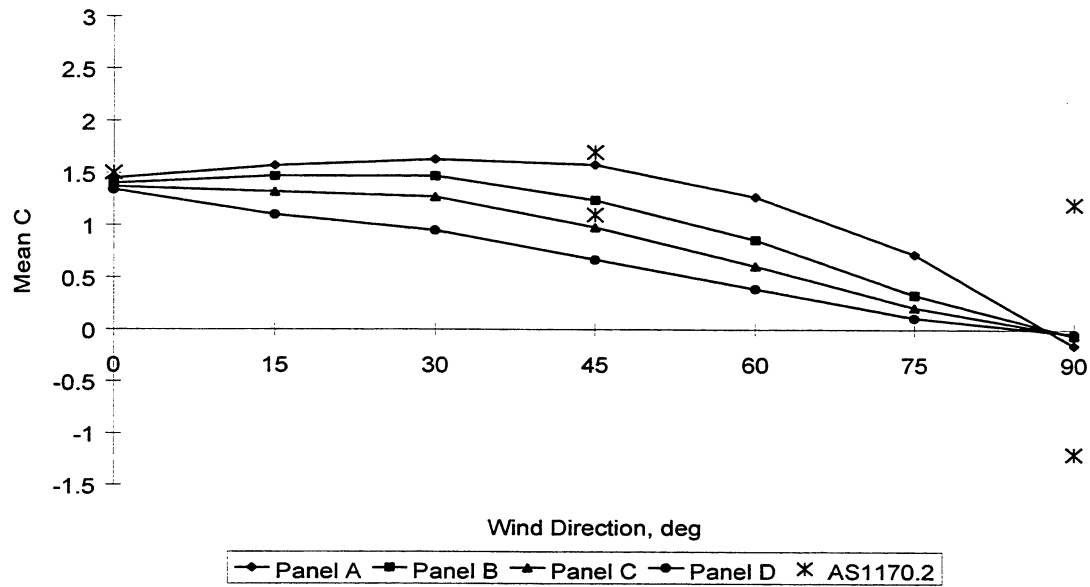


Figure 4.11 C_{pn} vs θ on hoarding panels $b/h = 2$, $c/h = 0.57$

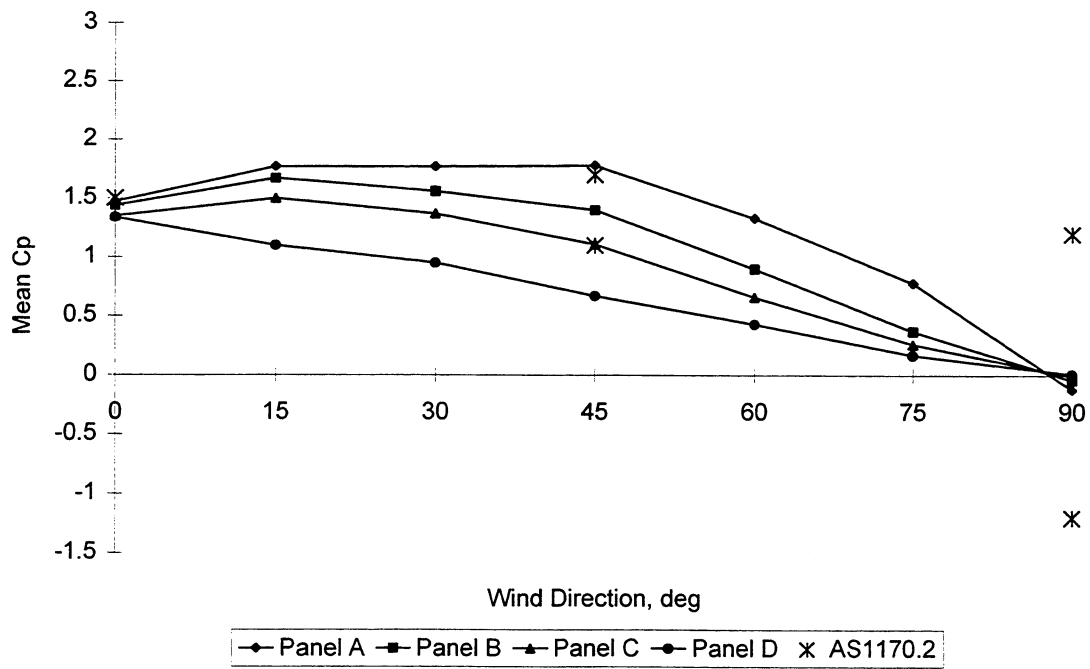


Figure 4.12 C_{pn} vs θ on hoarding panels $b/h = 2$, $c/h = 0.67$

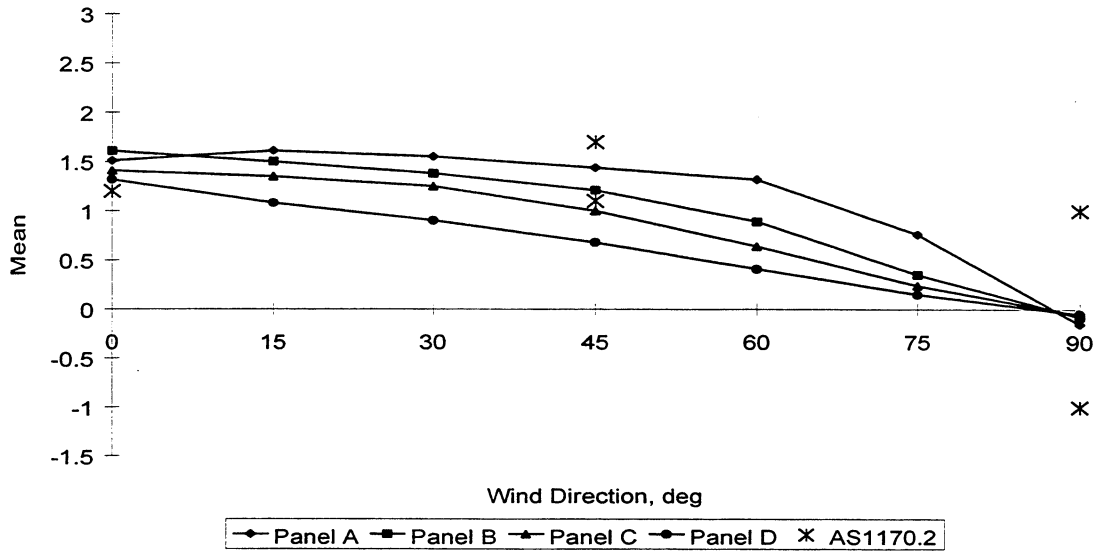


Figure 4.13 C_{pn} vs θ on hoarding panels $b/h = 2$, $c/h = 0.80$

The area averaged mean net pressure coefficients on $b/2$ wide parts of the hoarding (with a fixed aspect ratio $b/c = 2$) vs clearance ratio c/h , from the CSTS study and codes, for $\theta = 0^\circ$ and 45° are given in Tables 4.4 and 4.5 respectively. For $\theta = 0^\circ$, the region 0 to $b/2$ from the free-end is symmetrical to the region $b/2$ to b from the free-end and the CSTS results are derived by averaging the mean pressures on panels A, B, C and D. Table 4.4 for $\theta = 0^\circ$ shows that the mean net pressure coefficient on the hoarding with an aspect ratio $b/c = 2$ is underestimated by AS1170.2 for a clearance ratio, c/h of 0.8. ENV 1991-2-4 specifies that the force acts at a height of the center of the hoarding, at a distance of $0.25b$ from the vertical line passing through the center.

Table 4.4 Mean net pressure coefficients vs clearance ratio c/h on hoarding, $b/c = 2$ and $\theta = 0^\circ$

	Mean net pressure coefficients $\theta = 0^\circ$							
	CSTS Study		AS1170.2		ASCE 7-95		ENV 1991-2-4	
Distance from Windward free-end	0 to $b/2$	$b/2$ to b	0 to $b/2$	$b/2$ to b	0 to $b/2$	$b/2$ to b	0 to $b/2$	$b/2$ to b
$c/h = 0.57$	1.39	1.39	1.5	1.5	1.2	1.2	1.56	1.56
$c/h = 0.67$	1.39	1.39	1.5	1.5	1.2	1.2	1.56	1.56
$c/h = 0.80$	1.43	1.43	1.2	1.2	1.2	1.2	1.56	1.56

Table 4.5 Mean net pressure coefficients vs clearance ratio c/h on hoarding, $b/c = 2$ and $\theta = 45^\circ$

	Mean net pressure coefficients $\theta = 45^\circ$							
	CSTS Study		AS1170.2		ASCE 7-95		ENV 1991-2-4	
Distance from Windward free-end	0 to $b/2$	$b/2$ to b	0 to $b/2$	$b/2$ to b	0 to $b/2$	$b/2$ to b	0 to $b/2$	$b/2$ to b
$c/h = 0.57$	1.41	0.83	1.7	1.1	1.2	1.2	1.56	1.56
$c/h = 0.67$	1.59	0.95	1.7	1.1	1.2	1.2	1.56	1.56
$c/h = 0.80$	1.33	0.84	1.7	1.1	1.2	1.2	1.56	1.56

Letchford (1998) showed that for $\theta = 0^\circ$, the mean net pressure coefficient on the hoarding increases as the clearance ratio (c/h) was decreased and that this effect was more pronounced as the aspect ratio (b/c) was increased to 10. Table 4.6 compares the mean net pressure coefficient on hoardings with a range of clearance ratios, (c/h) obtained from this CSTS study with Equation 2.1 proposed by Letchford (1998) to describe the mean normal force coefficient on a hoarding.

Table 4.6 Mean net pressure coefficients on entire hoarding vs clearance ratio c/h
hoarding, $b/c = 2$ and $\theta = 0^\circ, 45^\circ$

	Mean net pressure coefficients		
	CSTS Study		Equation 2.1, Letchford (1998)
	$\theta = 0^\circ$	$\theta = 45^\circ$	$\theta = 0^\circ$
$c/h = 0.57$	1.39	1.12	1.41
$c/h = 0.67$	1.39	1.27	1.37
$c/h = 0.80$	1.43	1.08	1.30

5 DESIGN REQUIREMENTS OF FENCES

The components of a typical boundary fence are shown in Figure 5.1. The design wind loads and the structural performance requirements of typical boundary fences constructed from impermeable infill panels attached to railings that are connected to fence posts, are determined in this section. This will enable manufacturers evaluate fence systems and to construct fences suitable for a range of wind climates. Langtree (1997) showed that the pressure fluctuations on the fence over panel widths of $2h$ were almost fully correlated. This confirms Letchford's (1985) assertion that the quasi-static method can be satisfactorily used for determining the wind loads on fences and hoardings. Design wind load effects are calculated using the wind tunnel data and compared with values obtained from using AS1170.2.

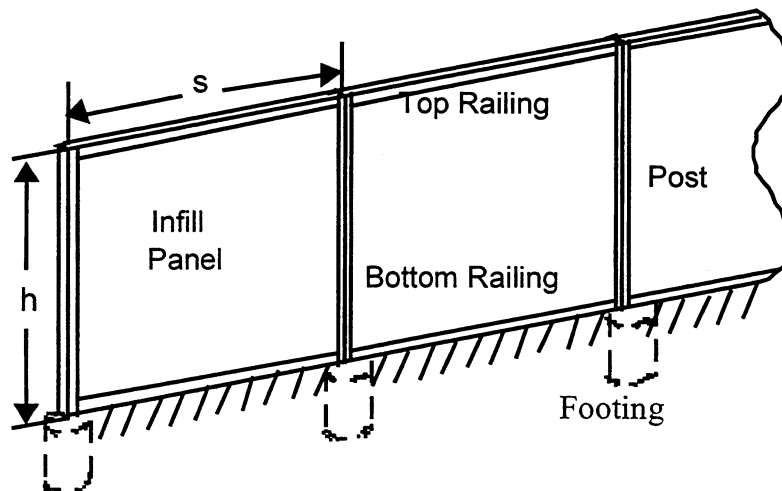


Figure 5.1 Components of a typical boundary fence

The design load effects are determined on a 1.8 m high \times 10.8 m long fence (i.e. aspect ratio 6) using the wind tunnel data for wind directions of 0° and 30° , and using AS1170.2 data for $\theta = 0^\circ$ and 45° . The fence posts are placed at 2.7 m (i.e. 1.5h) intervals, which is also the span of the top and bottom railings and the width of the infill panel bays.

The design pressure on infill panels are derived from the quasi-static method of Equation 5.1, which is similar to the approach used in AS1170.2.

$$\bar{p}_n = C_{pn} \left(\frac{1}{2} \rho \bar{U}_h^2 \right) \quad 5.1$$

Here \bar{U}_h is the gust wind speed at the fence height h. Assuming that the fence is to be installed in cyclone region C as per AS1170.2, the ratio of gust wind speed at 1.8m (i.e. fence height) in terrain category 3 to the gust wind speed at 10m in terrain category 2 obtained from Table 3.2.5.2 in AS1170.2 is $(\bar{U}_{1.8mTC3} / \bar{U}_{10mTC2}) = 0.8$. The basic ultimate limit state design wind speed of 70 m/s therefore gives $\bar{U}_{1.8mTC3} = 0.8 \times 70 = 56$ m/s. The design pressure in kPa is $\bar{p}_n = C_{pn} \left(\frac{1}{2} \times 1.2 \times 56^2 \right) \times 10^{-3}$.

The net pressure coefficients C_{pn} on h/2 wide strips located within a distance 0 to 3h from the windward free end for the fence of aspect ratio b/h = 6, measured in the wind tunnel (i.e. Table A4 in Appendix A) and from Table 3.4.13 in AS1170.2 are given in Table 5.1.

Table 5.1 Pressure coefficients on h/2 wide panels for fence of aspect ratio b/h = 6

Panel	Distance from windward free-end	Area averaged mean pressure coefficient			
		AS1170.2		CSTS study	
		$\theta = 0^\circ$	$\theta = 45^\circ$	$\theta = 0^\circ$	$\theta = 30^\circ$
A _E	0-h/2	1.2	2.4	1.19	2.29
B _E	h/2 to h	1.2	2.4	1.27	2.10
C _E	h to 3h/2	1.2	2.4	1.19	1.74
D _E	3h/2 to 2h	1.2	2.4	1.11	1.43
A _M	2h to 5h/2	1.2	1.2	1.08	1.39
B _M	5h/2 to 3h	1.2	1.2	1.05	1.19

The pressures are assumed to act uniformly over each h/2 wide strips of the infill panel and the infill panels are considered to be simply supported between the railings at the top and bottom as shown in Figure 5.2. Pressures of p_{AE} , p_{BE} and p_{CE} acting on each h high \times h/2 wide strips of Infill Panel 1 (i.e. first panel from free-end) and imparts load of $p_{AE}h/2$, $p_{BE}h/2$ and $p_{CE}h/2$ in kN/mwidth on each railing.

The design bending moment at the mid-height C of Infill Panel 1 (i.e. first panel from free-end) in kNm/(mwidth) may be approximated by Eqn 5.2, where p_{AE} is the load on the end h/2 wide strip,

$$M_C = \frac{p_{AE} h^2}{8} \quad 5.2$$

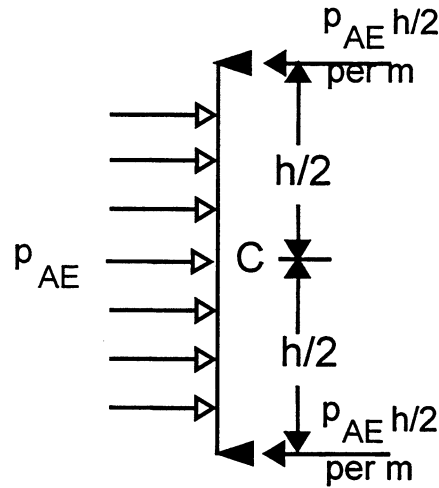


Figure 5.2 Wind loads per unit width on infill panel A

The top and bottom railings of span $s = 2.7$ m, are assumed to be simply supported at the fence posts. The distributed loads of $p_{AE}h/2$, $p_{BE}h/2$ and $p_{CE}h/2$ act on $h/2$ wide sections of the top and bottom railings supporting Infill Panel 1 as shown in Figure 5.3. The reactions on the railings by the first and second posts from the free-end are $R_{11} = \frac{h^2}{24}(5p_{AE} + 3p_{BE} + p_{CE})$ and $R_{12} = \frac{h^2}{24}(p_{AE} + 3p_{BE} + 5p_{CE})$ respectively.

The peak bending moment M_R in kNm, is at a distance $y_m = \frac{h}{12p_{BE}}(p_{CE} + 9p_{BE} - p_{AE})$ from the free-end

$$M_R = R_{11}y_m - \frac{h^2}{4}p_{AE}\left(y_m - \frac{h}{4}\right) - \frac{h}{4}p_{BE}\left(y_m - \frac{h}{2}\right)^2 \quad 5.3$$

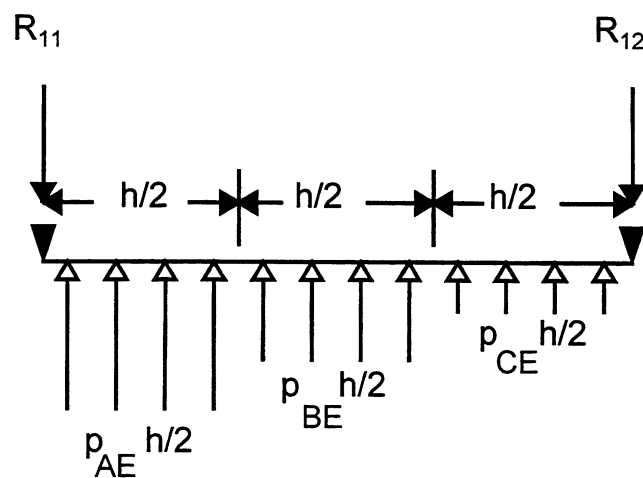


Figure 5.3 Loading distribution on top railing supporting panel A

The post foundation is assumed to provide the post with a fixed end restraint at the base. Loads are applied to the post by each rail as shown by Figure 5.4. The second post from the free end takes loads R_{12} and R_{22} from each top and bottom railing supporting Panels 1 and 2 respectively, and hence experiences higher loads than the post at the free-end which takes loads R_{11} from the railings supporting only Panel 1.

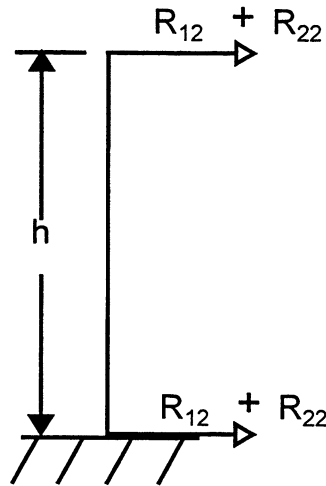


Figure 5.4 Loading distribution on second post from the windward free-end

The design shear force at the base of the second post from the free-end in kN

$$V_p = 2(R_{12} + R_{22}) = 2\left(\frac{h^2}{24}(p_{AE} + 3p_{BE} + 5p_{CE}) + \frac{h^2}{24}(5p_{DE} + 3p_{AM} + p_{BM})\right)$$

$$V_p = \frac{h^2}{12}(p_{AE} + 3p_{BE} + 5p_{CE} + 5p_{DE} + 3p_{AM} + p_{BM}) \quad 5.4$$

The design base overturning moment at the second post from the free end in kNm

$$M_p = \frac{h}{2}2(R_{12} + R_{22}) = h\left(\frac{h^2}{24}(p_{AE} + 3p_{BE} + 5p_{CE}) + \frac{h^2}{24}(5p_{DE} + 3p_{AM} + p_{BM})\right)$$

$$M_p = \frac{h^3}{24}(p_{AE} + 3p_{BE} + 5p_{CE} + 5p_{DE} + 3p_{AM} + p_{BM}) \quad 5.5$$

Table 5.2 Design wind load effects derived from wind tunnel data and AS1170.2

Design Load Effect	AS 1170.2		CSTS Wind Tunnel Study	
	$\theta = 0^\circ$	$\theta = 45^\circ$	$\theta = 0^\circ$	$\theta = 30^\circ$
M_C (kNm/mwidth)	0.91	1.83	0.91	1.75
M_R (kNm)	1.85	3.70	1.90	3.34
V_p (kN)	10.98	21.95	10.26	15.14
M_p (kNm)	9.88	19.75	9.51	13.26

Table 5.2 shows that the design load effects derived from wind tunnel data generally compare favourably with the values obtained from using AS1170.2. However, AS1170.2 may underestimate design load effects in the cases such as for aspect ratios of 4, 8 and 12, where the wind tunnel results were larger than the AS1170.2 values.

6 CONCLUSIONS

A wind tunnel model study was carried out to determine net pressures on a range of fence and hoarding configurations. These measured pressure distributions were compared with data from other studies and codified values. The pressure data were also used to identify fence and hoarding configurations and local regions experiencing large loads. The following conclusions were reached from this study.

- For an approach wind direction $\theta = 0^\circ$, the mean net pressure coefficient over the entire fence decreased as the aspect ratio was increased to ~ 5 in agreement with other model studies.
- Large area averaged mean net pressure coefficients were measured on windward free-end panels (up to a distance of $2h$) of the fence, for an approach wind direction θ of 30° to 45° .
- The area averaged mean net pressure coefficients on windward free-end panels (up to a distance of $2h$) of the fence, increased as the aspect ratio was increased to 8, and then decreased as the aspect ratio was increased to 12.
- The area averaged net pressure coefficients measured on the windward free-end panels (up to a distance of h) for fences of aspect ratios of 4, 8 and 12 for approach wind directions θ of 30° to 45° were larger than the values given in AS1170.2 for $\theta = 45^\circ$.
- The net pressure coefficients (i.e. the mean force coefficients) measured on a hoarding with an aspect ratio of 2 and clearance ratios (c/h) 0.57 and 0.67 were in good agreement with other model studies and AS1170.2. However, other codes such as ASCE 7-95 and ISO 4354 indicated some discrepancies.

7 REFERENCES

1. Australian Standard AS 1170.2-1989, SAA Loading Code Part 2: Wind Loads
2. ASCE Standard, ANSI/ASCE 7-95, Minimum Design Loads for Buildings and Other Structures, 1996
3. British Standards Institution, BS 6399: Loading for Buildings Part 2: Code of Practice for Wind Loading, 1995
4. ESDU International, Boundary Walls, Fences and Hoardings: Mean and Peak Wind Loads and Overturning Moments, Data Item 89050, 1989
5. European Prestandard, ENV 1991-2-4, Eurocode 1: Basis of Design and Action on Structures, Part 2.4: Wind Actions
6. M. C. Good and P. N. Joubert, "The Form Drag of Two-Dimensional Bluff-Plates Immersed in Turbulent Boundary Layers", Jour. of Fluid Mech., Vol. 31, Part 3, pp 547-582, 1968
7. J. D. Holmes, "Wind Loading on Free Standing Walls" Internal Report 85/13, CSIRO Division of Building Research 1985
8. International Standard ISO 4354, Wind Action on Structures, 1997

9. B. A. Langtree, (1997), "Wind Loads on Free Standing Walls and Hoardings" BE Thesis, Dept. of Civil & Environmental Engineering, James Cook Uni., Townsville Australia
10. C. W. Letchford, (1985), "Wind Loads on Free Standing Walls" OUEL Report 1599/85, Dept. of Engineering Science, Oxford University, UK.
11. C. W. Letchford and J. D. Holmes, (1994), "Wind Loads on Free Standing Walls in Turbulent Boundary Layers" Jour. of Wind Engg. & Indus. Aero., Vol. 51 pp 1-27
12. C. W. Letchford and A. P Robertson, (1998), "Mean Wind Loading at the Leading Ends of Free Standing Walls" Accepted for Publication in Jour. of Wind Engg. & Indus. Aero.
13. C. W. Letchford, (1998), "Wind Loads on Rectangular Signboards and Hoardings" Submitted to Jour. of Wind Engg. & Indus. Aero.
14. K. G. Raga Raju, J. Loeser and E. J. Plate, (1976), "Velocity Profiles and Fence Drag for a Turbulent Boundary Layer along Smooth and Rough Plates", Jour. of Fluid Mech., Vol. 70, Part 2, pp 383-399
15. A. P Robertson, R. P Hoxey and P. J. Richards, (1995), "Design Code, Full-Scale and Numerical Data for Wind Loads on Free Standing Walls" Jour. of Wind Engg. & Indus. Aero., Vol. 57 pp 203-214
16. A. P Robertson, R. P Hoxey, J. L Short, W. A Ferguson and P. A. Blackmore, (1997), "Wind Loads on Boundary Walls: Full-Scale Studies" Jour. of Wind Engg. & Indus. Aero., Vol. 69-71 pp 451-459
17. H. Sakamoto and M. Arie, (1983), "Flow Around a Normal Flat Plate Immersed in a Turbulent Boundary Layer", Jour. of Fluids Engg., ASME Trans. Vol. 105, pp, 98-104

APPENDIX A MEAN PRESSURE COEFFICIENTS

Table A.1 Mean net pressure coefficients vs wind direction on fence, $b/h = 2$

	Mean Pressure Coefficient						
θ (°)	0	15	30	45	60	75	90
Panel A	1.29	1.38	1.42	1.43	1.25	0.75	-0.20
Panel B	1.31	1.38	1.33	1.26	1.02	0.37	-0.09
Panel C	1.27	1.22	1.16	0.98	0.68	0.22	-0.02
Panel D	1.15	0.93	0.81	0.64	0.39	0.12	-0.01
AS1170.2	1.2			(0 - b/2) 1.7 (b/2 - b) 1.1			± 1.0

Table A.2 Mean net pressure coefficients vs wind direction on middle section of fence, $b/h = 4$

	Mean Pressure Coefficient						
θ (°)	0	15	30	45	60	75	90
Panel A _M	1.12	1.34	1.49	1.30	0.79	0.27	-0.04
Panel B _M	1.05	1.17	1.22	1.01	0.58	0.18	-0.05
Panel C _M	1.08	1.07	1.01	0.87	0.53	0.16	-0.03
Panel D _M	1.11	0.97	0.82	0.73	0.45	0.13	-0.03
AS1170.2	1.2			(0 - b/2) 1.7 (b/2 - b) 1.1			± 1.0

Table A.3 Mean net pressure coefficients vs wind direction on free-end section of fence, $b/h = 4$

	Area Averaged Mean Pressure Coefficient												
θ (°)	-90	-75	-60	-45	-30	-15	0	15	30	45	60	75	90
Panel A _E	-0.01	0.31	0.77	1.06	1.20	1.18	1.16	1.42	1.84	1.98	1.39	0.82	-0.18
Panel B _E	-0.01	0.26	0.65	0.89	1.02	1.08	1.16	1.41	1.77	1.77	1.18	0.45	-0.12
Panel C _E	-0.02	0.21	0.52	0.70	0.87	1.01	1.12	1.33	1.54	1.36	0.83	0.28	-0.08
Panel D _E	-0.01	0.14	0.32	0.45	0.64	0.84	1.06	1.20	1.28	1.07	0.65	0.22	-0.08
AS1170	± 0.5			1.1			1.2			1.7			± 1.0

Table A.4 Mean net pressure coefficients vs wind direction on middle section of fence, $b/h = 6$

	Mean Pressure Coefficient						
θ (°)	0	15	30	45	60	75	90
Panel A _M	1.11	1.30	1.39	1.19	0.76	0.30	-0.03
Panel B _M	1.05	1.19	1.19	0.99	0.65	0.26	-0.04
Panel C _M	1.04	1.12	1.06	0.88	0.60	0.25	-0.03
Panel D _M	1.05	1.05	0.94	0.77	0.54	0.23	-0.03
AS1170.2	1.2			(2h - 4h) 1.2			± 0.5

Table A.5 Mean net pressure coefficients vs wind direction on free-end section of fence, $b/h = 6$

	Area Averaged Mean Pressure Coefficient												
θ (°)	-90	-75	-60	-45	-30	-15	0	15	30	45	60	75	90
Panel A _E	-0.04	0.28	0.57	0.76	0.88	0.99	1.19	1.57	2.29	2.19	1.47	0.72	-0.11
Panel B _E	-0.04	0.25	0.49	0.64	0.80	0.96	1.27	1.56	2.10	1.94	1.24	0.44	-0.10
Panel C _E	-0.05	0.20	0.40	0.53	0.71	0.93	1.19	1.45	1.74	1.38	0.86	0.29	-0.05
Panel D _E	-0.02	0.13	0.25	0.35	0.53	0.81	1.11	1.30	1.43	1.19	0.72	0.23	-0.06
AS1170	± 0.25			0.6			1.2			2.4			± 1.0

Table A.6 Mean net pressure coefficients vs wind direction on middle section of fence, $b/h = 8$

	Mean Pressure Coefficient						
θ (°)	0	15	30	45	60	75	90
Panel A _M	1.28	1.40	1.29	1.10	0.69	0.24	-0.03
Panel B _M	1.23	1.31	1.17	0.96	0.63	0.21	-0.04
Panel C _M	1.23	1.26	1.09	0.89	0.59	0.22	-0.02
Panel D _M	1.24	1.21	1.02	0.82	0.56	0.21	-0.03
AS1170.2	1.2			(2h-4h) 1.2 (>4h) 0.6			(2h-4h)±0.5 (>4h) ±0.25

Table A.7 Mean net pressure coefficients vs wind direction on free-end section of fence, $b/h = 8$

	Area Averaged Mean Pressure Coefficient												
θ (°)	-90	-75	-60	-45	-30	-15	0	15	30	45	60	75	90
Panel A _E	0.00	0.23	0.51	0.68	0.91	1.10	1.38	2.01	2.93	2.74	1.77	0.99	-0.10
Panel B _E	0.00	0.22	0.45	0.61	0.86	1.07	1.46	2.04	2.71	2.41	1.54	0.56	-0.08
Panel C _E	-0.01	0.17	0.36	0.53	0.78	1.07	1.41	1.89	2.24	1.78	1.08	0.39	-0.04
Panel D _E	0.01	0.11	0.24	0.36	0.59	0.94	1.31	1.71	1.90	1.58	0.90	0.33	-0.05
AS1170	± 0.25			0.6			1.2			2.4			± 1.0

Table A.8 Mean net pressure coefficients vs wind direction on middle section of fence, $b/h=12$

	Mean Pressure Coefficient						
θ (°)	0	15	30	45	60	75	90
Panel A _M	1.37	1.38	1.25	1.03	0.64	0.25	-0.01
Panel B _M	1.32	1.32	1.20	0.98	0.61	0.23	-0.02
Panel C _M	1.28	1.28	1.18	0.95	0.59	0.23	-0.01
Panel D _M	1.29	1.25	1.13	0.89	0.56	0.20	-0.02
AS1170.2	1.2			(>4h) 0.6			(>4h) ±0.25

Table A.9 Mean net pressure coefficients vs wind direction on free-end section of fence $b/h = 12$

	Area Averaged Mean Pressure Coefficient												
θ (°)	-90	-75	-60	-45	-30	-15	0	15	30	45	60	75	90
Panel A _E	-0.06	0.21	0.44	0.66	0.92	0.98	1.22	1.90	2.60	2.37	1.43	0.88	-0.05
Panel B _E	-0.06	0.18	0.38	0.61	0.84	0.95	1.28	1.89	2.30	2.07	1.18	0.51	-0.05
Panel C _E	-0.06	0.15	0.32	0.54	0.77	0.92	1.15	1.74	1.87	1.58	0.78	0.34	-0.03
Panel D _E	-0.03	0.10	0.21	0.38	0.56	0.80	1.10	1.58	1.58	1.44	0.62	0.28	-0.04
AS1170	±0.25			0.6			1.2			2.4			± 1.0

Table A.10 Mean net pressure coefficients vs wind direction on hoarding $b/c=2$, $c/h = 0.57$

	Mean Pressure Coefficient						
θ (°)	0	15	30	45	60	75	90
Panel A	1.45	1.57	1.63	1.58	1.27	0.72	-0.15
Panel B	1.40	1.47	1.47	1.24	0.86	0.33	-0.06
Panel C	1.37	1.32	1.27	0.98	0.61	0.21	-0.05
Panel D	1.34	1.10	0.95	0.67	0.39	0.11	-0.04
AS1170.2	1.5			(0 - b/2) 1.7 (b/2 - b) 1.1			± 1.2

Table A.11 Mean net pressure coefficients vs wind direction on hoarding $b/c=2$, $c/h = 0.67$

	Mean Pressure Coefficient						
θ (°)	0	15	30	45	60	75	90
Panel A	1.47	1.77	1.77	1.78	1.33	0.78	-0.12
Panel B	1.44	1.67	1.56	1.40	0.90	0.37	-0.04
Panel C	1.35	1.50	1.37	1.11	0.66	0.26	-0.01
Panel D	1.31	1.25	1.02	0.79	0.43	0.17	0.01
AS1170.2	1.5			(0 - b/2) 1.7 (b/2 - b) 1.1			± 1.2

Table A.12 Mean net pressure coefficients vs wind direction on hoarding $b/c=2$, $c/h = 0.80$

	Mean Pressure Coefficient						
θ (°)	0	15	30	45	60	75	90
Panel A	1.51	1.61	1.55	1.44	1.32	0.76	-0.15
Panel B	1.47	1.50	1.38	1.21	0.89	0.35	-0.08
Panel C	1.41	1.35	1.25	1.00	0.64	0.24	-0.06
Panel D	1.32	1.08	0.90	0.68	0.41	0.15	-0.05
AS1170.2	1.2			(0 - b/2) 1.7 (b/2 - b) 1.1			± 1.0